

Magnetic Field Effects on pH and Electrical Conductivity: Implications for Water and Wastewater Treatment

Tao Wu, and Jonathan A. Brant^{*,†}

Department of Civil and Architectural Engineering, University of Wyoming, Laramie, Wyoming, USA.

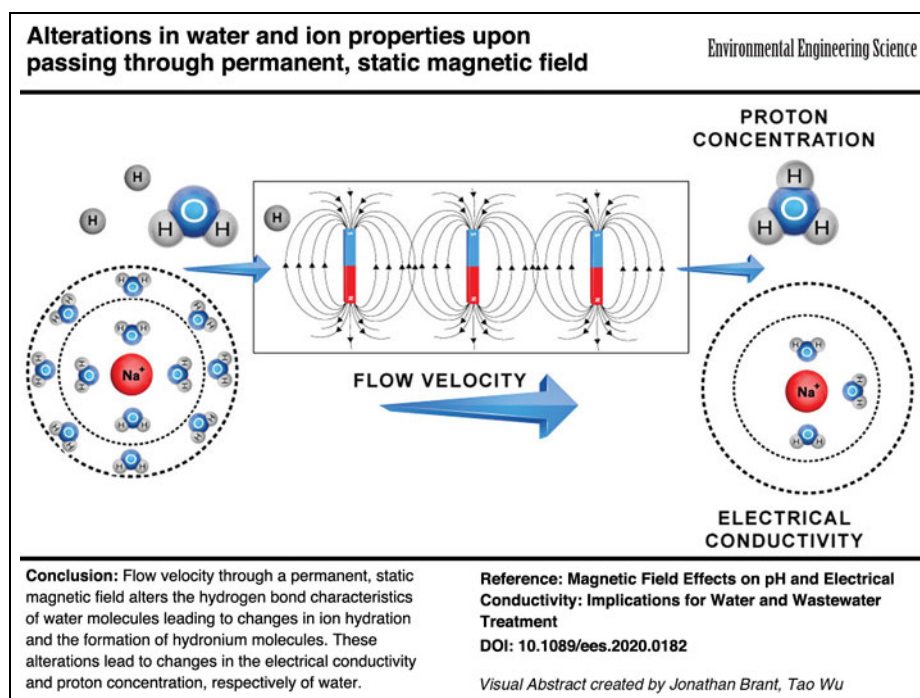
Received: May 8, 2020

Accepted in revised form: July 13, 2020

Abstract

Manipulation of water chemistry plays an important role in water and wastewater treatment. Much effort has been directed at accomplishing such changes in ways that require less energy and material consumption to reduce treatment costs and improve process sustainability. Magnetic fields have been shown to affect the properties of water and its constituents. In this study, theoretical assessments of changes in electrical conductivity and proton concentration, as a function of flow velocity through a magnetic field, were developed and experimentally verified. Experiments were done using a flow-through system consisting of permanent neodymium magnets arranged in a helical pattern in a pipe to generate a constant multidirectional magnetic field (1.350 T). In accordance with increasing flow velocity (8–6 cm/s), the proton concentration decreased from 10^{-7} to 6×10^{-8} mol/L (pH 7–7.22). The model developed in this study indicated that pH would increase from 7 to 14 at a velocity of 100 cm/s. Change of electrical conductivity increased by 100 to 250 $\mu\text{S}/\text{cm}$ with increasing flow velocity. The decrease in proton concentration was due to an increase in hydrogen bonding between water molecules and protons. Electrical conductivity was increased due to weakening of the hydration shells around the constituent ions and an increase in the internal electrical field.

Graphical Abstract



Keywords: electrical conductivity; magnetic field; magnetic treatment; pH; proton concentration; water treatment

*Corresponding author: Department of Civil and Architectural Engineering, University of Wyoming, 1000 E University Avenue, Laramie, WY 82071, USA. Phone: 307-766-5446; Fax: 307-766-7221; E-mail: jbrant1@uwyo.edu

[†]Member of AEESP.

Introduction

THE WORLD FACES a growing water crisis due to exponential population growth, climate change, finite freshwater supplies, and other factors (Ashoori *et al.*, 2017). Additional concerns have been raised regarding the safety of potable water supplies with regard to the presence of unwanted compounds, like disinfection byproducts (Ding *et al.*, 2019), and emerging contaminants of concern (Wee and Aris, 2017). Entry routes for these materials into water systems are diverse and may be intentional or unintentional. Conventional water and wastewater treatment systems use chemical additives to alter water chemistry and/or affect the behavior of water constituents. While effective, the usage of chemicals is associated with a variety of drawbacks like cost, the generation of unwanted byproducts, and health and safety concerns for operators. Development of processes that can supplement, or replace, the need for chemical addition is therefore of interest to the water management stakeholders. Devices that rely on magnetic fields for altering the properties of materials, like water, are emerging, and exciting technologies that may alter how water is treated in the future. Of relevance to this work, is that magnetic devices are not reliant on physical barriers or chemical additives to affect changes in system characteristics.

Magnetic fields have been shown to affect the characteristics of water, like pH and electrical conductivity, and its constituents (Quickenden *et al.*, 1971; Yamashita *et al.*, 2003; Cai *et al.*, 2009; Szcześ *et al.*, 2011b; Ebrahimi and Saghavani, 2017; Wang *et al.*, 2018; Liu *et al.*, 2019). These observations are generally ascribed to changes in the strength and/or number of hydrogen bonds between water molecules and water molecules and ions. Important characteristics of the magnetic field in these applications include strength, or flux density, of the magnetic field, B , magnetic field gradient, ΔB , and residence time within the magnetic field, t_h . Upon exposure to a magnetic field, the total conformation energy of a molecular system is altered (Levitt *et al.*, 1997; Spreiter and Walter, 1999; Wu *et al.*, 2006). These alterations consist of the energy differences introduced by individual bonding, bending, van der Waals, and Coulomb potentials. With changes in energy, the distance between an oxygen atom of a molecule and a hydrogen atom of another molecule will be altered accordingly. If the distance is shortened, hydrogen bonds will be formed/strengthened, and if the distance is prolonged, the hydrogen bonds are eliminated/weakened. And as reported by Chang and Weng (2006, 2008), when exposed to magnetic fields, the distance was decreased and more hydrogen bonds were formed. Numerous researchers have observed how magnetic fields can alter the properties of water.

Cai *et al.* (2009) observed that the application of $B = 10$ to 1,000 mT for 15 min, to water stream increased its viscosity from 1.07 to 1.18 mPa/s, resulting from an increase in the Lorentz force, which comprised electrical and magnetic forces. Yamashita *et al.* (2003) studied the effects of two different types of magnetic fields on pH and oxidation reduction potential (ORP). They found that the pH fluctuated by ~ 0.05 to 0.1 pH units and the ORP fluctuated by roughly ~ 60 mV following several hours of exposure. In a similar study, Chibowski *et al.* (2005) observed an increase in pH (~ 0.25 pH units) as a function of exposure time (0–10 min)

at $B = 0.27$ T. Changes in hydrogen bonding were referenced as the source of the observed pH effects. Szcześ *et al.* (2011b) found that circulating water through a magnetic field ($B = 0.27$ T) for 5 min resulted in a decrease (~ 0.125 $\mu\text{S}/\text{cm}$) in its electrical conductivity. This relationship was a function of t_h , although the authors did not postulate on the underlying mechanisms. Contrasting observations were made by Holysz *et al.* (2007), who studied the changes in electrical conductivity when exposed to a static (no flow) magnetic field ($B = 0.015$ T). Electrical conductivity increased indicating that the presence of a ΔB may play a role in determining how the conductivity changes. The authors hypothesized that changes in electrical conductivity were due to weakening of the hydration shells around proton, hydroxide, potassium, and chloride ions. Since electrical conductivity is inversely proportional to the diameter of the hydrated cation or anion, and when the hydration shell is weakened/distorted by the magnetic field, the conductivity of a solution is increased (Chibowski *et al.*, 2005). There is supporting evidence from other works to support the idea that magnetic fields can affect hydrogen bonding between water molecules and ions.

Pang and Feng (2003) developed a theoretical construct for describing the relationship between magnetic fields and water structuring at the quantum and molecular scales. These changes in water structuring were used to describe experimental observations in terms of ion mobility in water and the solution electrical conductivity. Cai *et al.* (2009) reported that hydrogen bonding between water molecules was enhanced when exposed to a magnetic field ($B = 0.5$ T). This was attributed to the effect of the Lorentz force on protons and promoting their bonding to water to form hydronium (H_3O^+). Wang *et al.* (2013) also found that at a fixed temperature (300 K), a magnetic field ($B = 0.27$ T) increased the number of hydrogen bonds in a solution. Supporting observations were made by Pang and Deng (2008), who observed that the Raman absorption at $6,000\text{ cm}^{-1}$ shifted from 0 to 90,000 (unitless). An increased Raman absorption indicated that the structure arrangements of water molecules were changed, and an increase occurred in hydrogen bonds between water molecules and between water molecules and hydronium. This finding was supported by Chang *et al.* (2006) who using molecular dynamics simulations, determined that the number of hydrogen bonds increased in the presence of a magnetic field ($B = 1$ T).

There exist important knowledge gaps in our understanding of how magnetic fields affect water properties. In this work, we studied the role that velocity through a magnetic field plays in determining changes in proton concentration (pH) and electrical conductivity. Both water properties are important in water/wastewater treatment applications. The former is particularly important as it is commonly manipulated to affect the solubility of metal salts (coagulation) and minerals (hardness removal), and stabilizing water post-acidification. Flow velocity is important as it directly affects the magnitude of the Lorentz Force. Models were developed, and experimentally verified, for describing how flow velocity through a magnetic field determined the magnitude of change in water proton concentration (pH) and electrical conductivity. We found that when a constant external magnetic field is applied, electrical conductivity increased proportional to flow velocity, while proton concentration (pH) decreased inversely proportional to the velocity.

Theoretical

Assessment of changes in electrical conductivity

Elucidating the roles of, and relationships between, flow velocity through a magnetic field and electrical conductivity of water was theoretically evaluated in terms of an electromagnetic force [Eq. (1)].

$$F = \sum_n \frac{1}{4\pi\epsilon_0} \frac{q_0 q_n u_{rn}}{r_n^2} = qE_f + qvB \quad (1)$$

where F was the sum of the total electromagnetic forces acting on those substances moving through the magnetic field; n was the number of ionic substances; q_0 was the charge of a proton beam particle, q_n was the charge of the unit of the substances, u_r was a vector of unit length aligned along the force directed from one moiety to another; r is the force between two charged substance; u_{rn} was the vector to the specified substance; and ϵ_0 is absolute dielectric constant of water. The ionic composition of the water was not changed by the tested system (Supplementary Table S1) and so n was assumed to be constant. The number of charged substances may be variable as water molecules may be transformed, for example, to hydronium, or structurally rearrange themselves (Pang and Deng, 2008); however, these changes in the number of charged substances, and the subsequent intersubstance forces, could be considered negligible because the force between one to another changed accordingly (Pang, 2006).

E_f was used to represent the electric field generated by internal electric field generated by all substances moving through the magnetic field (Pang, 2006). Rearranging Equation (1) results in an expression for the internal electric field provided by all substances moving through the magnetic field, E_f [Eq. (2)].

$$E_f = \frac{\sum_n \frac{1}{4\pi\epsilon_0} \frac{q_0 q_n u_{rn}}{r_n^2}}{q} - vB \quad (3)$$

Because $\frac{\sum_n \frac{1}{4\pi\epsilon_0} \frac{q_0 q_n u_{rn}}{r_n^2}}{q}$ was constant, E_f was inversely proportional to velocity through the magnetic field. The relationship between the electrical field and the introduced electrical conductivity of the solution σ is shown in Equation (4).

$$nqv_d = \sigma E_f \quad (4)$$

where v_d was the drift speed, a constant, which is an instinct velocity after collision between charged substances in the absence of an external electrical field. The expression for electrical conductivity is given in Equation (5).

$$\frac{nqv_d}{\frac{\sum_n \frac{1}{4\pi\epsilon_0} \frac{q_0 q_n u_{rn}}{r_n^2}}{q} - vB} = \sigma \quad (5)$$

Using Equation (5), the electrical conductivity of a solution may be plotted as a function of flow velocity (Supplementary Fig. S1). Here, σ increases in a linear manner with velocity, however, when the velocity exceeds a certain threshold value [potentially 10% of speed of light, when

Newtonian mechanics starts to present error (Woodhouse, 2003), $v = 0.10c = 2.99792458 \times 10^7$ m/s]. Equation (5) was used to elucidate, and theoretically describe, the relationships between electrical conductivity and flow velocity through a magnetic field.

Assessment of changes in proton concentration

Energy introduced into the water by the magnetic field, $E(B)$, was calculated according to Equation (6) (Kusminskiy, 2019).

$$E(B) = -\frac{S_0^2}{2} \sum_{ij} J_{ij} - g\mu_B BNS \quad (6)$$

where B was the strength of the magnetic field ($= 1.350$ T); S_0 was the uniform angular momentum, or spin, through the system at constant temperature; J_{ij} was the exchange coefficient for each solute in water; g was the dimensionless magnetic moment; μ_B was the permeability of the permanent neodymium magnets; S was total momentum of substances moving through the magnetic field; and N was number of lattice sites (Kusminskiy, 2019). The value of $g\mu_B BNS$ is a linear function of the flow velocity through the magnetic field (Luengo-Kovac, 2017). Since the energy computed using Equation (6) was done at the quantum mechanics scale and could not reveal the relationship between the energy and velocity (Kusminskiy, 2019), the relativistic relationship between kinetic energy and momentum was introduced to form Equation (7).

$$E = \sqrt{p^2 c^2 + m^4 c^4} - mc^2 \quad (7)$$

Equation (7) was expanded and expressed as a Taylor series approximation [Eq. (8)]. Equation (8) shows how molecular mechanics may be combined with Newtonian mechanics when water molecules were considered collectively,

$$E \approx \frac{p^2}{2m} - \frac{p^4}{8m^3 c^2} \quad (8)$$

The energy of water molecules was dependent on the structure of the molecule and would be changed when temperature changed or other external energy was applied, and thus when external energy was considered another aspect, $-\frac{S_0^2}{2} \sum_{ij} J_{ij}$ of Equation (6), the internal energy $-\frac{S_0^2}{2} \sum_{ij} J_{ij}$ was considered constant. And although the external energy, $-g\mu_B BNS$ part of Equation (6), provided by moving through the magnetic field was through changing angular momentum of water molecule, it could be physiomathematically renormalized as linear momentum. Because, in this system, the radius of rotation could be considered going to infinity, which was from molecule scale to Newtonian mechanics scale, and, thus, the angular momentum could be renormalized as linear momentum, as shown in Equation (9).

$$L = mR^2 \omega = Rmv \quad (9)$$

where L represents the linear momentum; m is the mass of all substances; R is radius of rotation, and v is the velocity. In this

study, the radius of rotation is considered the inner diameter of the tube through which the water flows. Since Equations (7) and (8) support that potentiality, molecular mechanics could be correlated to Newtonian mechanics, the total angular momentum S in Equation (6) is substituted with Rmv in Equation (9) to form Equation (10).

$$E(B) = -\frac{S_0^2}{2} \sum_{ij} J_{ij} - g\mu_B \text{BNR}mv \quad (10)$$

The energy $E(B)$, introduced by the magnetic field, increases linearly with flow velocity.

The change in proton concentration resulting from flow through the magnetic field was calculated using Equation (11). With the conceived α and Equation (10), an equation could be built as Equation (11)

$$\Delta(H^+) = -\alpha \left(-\frac{S_0^2}{2} \sum_{ij} J_{ij} - g\mu_B \text{BNR}mv \right) \quad (11)$$

where $\Delta(H^+)$ is the change in proton concentration and α is the number of hydrogen bonds between water molecules and protons. α was determined from the linear slope of the measured proton concentration as a function of flow velocity.

Materials and Methods

Chemicals and reagents

All solutions were made using ultrapure water from a Milli-Q® Direct 16 water system (Millipore Sigma, Burlington, MA). The ultrapure water had a resistivity of 18 MΩ/cm and an unbuffered pH of 6.07 ± 0.05. Magnetic field experiments were done using tap water from the city of Laramie, WY. Representative water quality values for the tap water, measured over the course of the experiments, are given in Supplementary Table S2. The values reported in Supplementary Table S2 were collected for influent water samples used during the proton concentration and electrical conductivity experiments. The tap water in Laramie is characterized as relatively hard water with low total dissolved solid (TDS), characteristic of systems fed by a blend of ground and surface water. Citric acid (purity = 99.6%) and sodium chloride (purity ≥ 99.0%) were acquired from Fisher Scientific (Hampton, NH).

Analytical chemistry

Water samples were analyzed for major and minor ions using a Dionex Reagent-Free Ion Chromatograph (ICS-2100; Thermo Fisher Scientific; Waltham, MA). Samples were collected and stored in glass containers with screw top lids that had been acid washed before use. The organic content of water samples was determined in terms of the total organic carbon (TOC) concentration using a Sievers InnovOx ES Laboratory TOC Analyzer (Suez, Paris, France). TOC samples were collected in triplicate in precleaned glass vials. Turbidity was measured using a Micro 100 Laboratory Turbidimeter (HF Scientific, Inc., Fort Myers, FL).

Fourier transform infrared spectroscopy (FTIR) spectra were acquired by a Nicolet™ iS50 FTIR Spectrometer with an ATR module (Thermo Fisher Scientific). The infrared (IR) used for this study was mid-IR with a range of 4,000 to

500 cm⁻¹. For each measurement, 32 scans were performed. Before measurements for water samples, the spectrum of air was collected and used to correct that measured for the aqueous sample. To avoid potential effects introduced by changes of sample temperature, the FTIR spectra of the samples were acquired right after the water samples were collected ($T_{\text{avg}} = 13^\circ\text{C}$).

Nuclear magnetic resonance (NMR) transverse relaxation (T_2 relaxation) was conducted using a Bruker mq20 NMR spectrometer. The sample was filled in the instrument with a height of 1 cm as an optimum position for the probe chamber. The T_2 relaxation was measured by a standard Carr-Purcell-Meiboom-Grill pulse sequence. Here, 200 echoes, as well as an echo time of 14.21 μs were set to avoid the spin-locking effect. The number of scans used for this study was 32. The relaxation time was then obtained by the instruments with its provided software CONTIN. Also, T_2 relaxation analyses were performed right after the water samples were collected.

All analyses incorporated blanks and control samples in the sample matrix to ensure the accuracy of the measurements. All reported values represent the mean of a minimum of five measurements.

The magnetic field within the tubes that constituted the magnetic field test unit was modeled using Amperes 10.1 (Integrated Software, Manitoba, Canada). Amperes is a 3D modeling software that uses finite element methods to simulate the magnetic field strength as a function of system geometry and magnet characteristics. Simulations were done to characterize the magnetic field within the tubes as well as to ensure that the tubes were saturated with the magnetic field. For this study, the geometry, spatial arrangement, and properties of the N45 Grade NdFeB magnets were inputted into the software to visualize the resulting magnetic field in a single tube. When simulating the magnetic field, the simulation was set as finite with a direct matrix solver. For the simulations, the stainless-steel containers for the magnets were not included because they would not be magnetized, or affect the generated magnetic field, under the conditions used ($B \ll 1,000$ T). Other settings used during the simulations are summarized in Supplementary Table S3.

Flow-through magnetic field experiments

Magnetic field experiments were done using a pilot-scale test unit comprising three flow-through tubes linked in series and containing permanent neodymium magnets ($B = 1.350$ T, N45 Grade NdFeB). The magnets had a nickel chrome coating. The strength of magnetic field was measured using a Senis 3MTS 3-Axis USB Teslameter (GMW Associates, San Carlos, CA). The test unit was designated as the MFED system and was supplied by Strategic Environmental Solutions (Pensacola, FL). The magnets were sealed in machined stainless-steel tubular containers that were arranged in a helical pattern through a pipe. This spacing prevented the strength of the magnetic field from weakening to a non-saturation point before reaching another magnet (Supplementary Fig. S2). The helical arrangement of the magnets created a multidirectional magnetic field configuration. A multidirectional magnetic field prevented charged moieties from moving in only one direction, as well as preventing the creation of unidirectional attractive/repulsive forces from the magnetic field within their effective distance. When two

magnets are arranged with reverse poles directions, a charged moiety moving between the two fields would experience a unidirectional force, or no force at all (Supplementary Fig. S3a). Conversely, when a magnetic field generated by one magnet aligns with the poles of a second magnet, the two magnetic fields would have the same field direction and repel one another. Thus, there would be a zone within the effective area between the magnets that would lack a magnetic field (Supplementary Fig. S3b). Furthermore, charged moieties moving through this zone would not be impacted by magnetic field.

The process flow diagram for the MFED system is given in Fig. 1. This flow schematic is representative of how the actual system could be integrated into a full-scale water/wastewater treatment process. Essentially, no modifications to existing processes are required as the magnetic device is self-contained in the pipes. Only a change in the hydraulic flow path would be required, that is, the process would be piped into existing piping structures. The feed pump, pressure sensors (GC35; Ashcroft, Stratford, CT), and water quality probes (pH, electrical conductivity, dissolved oxygen, and free chlorine) were all connected to a computer for control and data acquisition through a LabView 2019 designed program. Sensors were acquired from HACH® (Loveland, CO) and were the following HACH models: pH (DPD1P1), conductivity (3700 Digital Inductive Conductivity Sensor), dissolved oxygen (LDO® Model 2), and free chlorine (CL 17). All probes were calibrated before each test. Sampling pumps acquired water samples for subsequent analysis on the influent and effluent flows for the MFED system. The hydraulic residence time of the MFED system was characterized using a sodium chloride tracer that was injected in the inlet to the MFED system. Influent and effluent samples for the tracer tests were collected from sample ports located on the immediate inlet and outlet from the MFED tubes. The electrical conductivities of these samples were measured

using a bench-top conductivity meter. Tracer tests were done at four different flow rates: 37.9, 75.7, 113.6, and 151.4 L/min. The tracer solution was dosed into the feed flow until the effluent conductivity varied by $\leq 5 \mu\text{S}/\text{cm}$. The hydraulic residence time was determined as the t_{10} time from C-plots for the conductivity data (Supplementary Fig. S4). From these tests, the system had mean residence times at the tested flow rates of 3.90, 1.97, 1.35, and 1.00 min.

All tests were done at a feed pH of 7, which was achieved using 0.1 M citric acid and 0.1 M sodium hydroxide dosing solutions. Free chlorine was quenched from the tap water using a 0.06 M sodium metabisulfite solution. Conductivity tests were done with an initial electrical conductivity of $1,000 \mu\text{S}/\text{cm}$, which was accomplished using 0.02 M sodium chloride dosing solution. The chemical dosing pumps were interfaced with online pH/free chlorine sensors for automatic adjustment. The temperature of the feed flow varied between 15.6°C and 16.8°C . Upon start-up, the system was flushed with tap water for a minimum of 30 min at a flow rate of 37.9 L/min to remove any air from the flow lines and to achieve the desired solution chemistry through the dosing systems. All probes remained in a wetted condition between tests. After the 30-min warm-up period, the test was initiated at the desired flow set-point. Water quality data were collected automatically every 10 s, apart from the free chlorine concentration, which was collected every 2.5 min.

Statistical analyses

Significance was assessed using a paired t -test analysis. Null hypothesis was postulated that the true mean difference is zero, $H_0 : \mu_d = 0$. Let x = one characteristic of the samples before magnetic treatment and y = the same characteristic of the samples after treatment. The difference, $d_i = y_i - x_i$, was then calculated. The mean difference, the point estimate of μ_d , \bar{d} was calculated. Standard error of the mean difference,

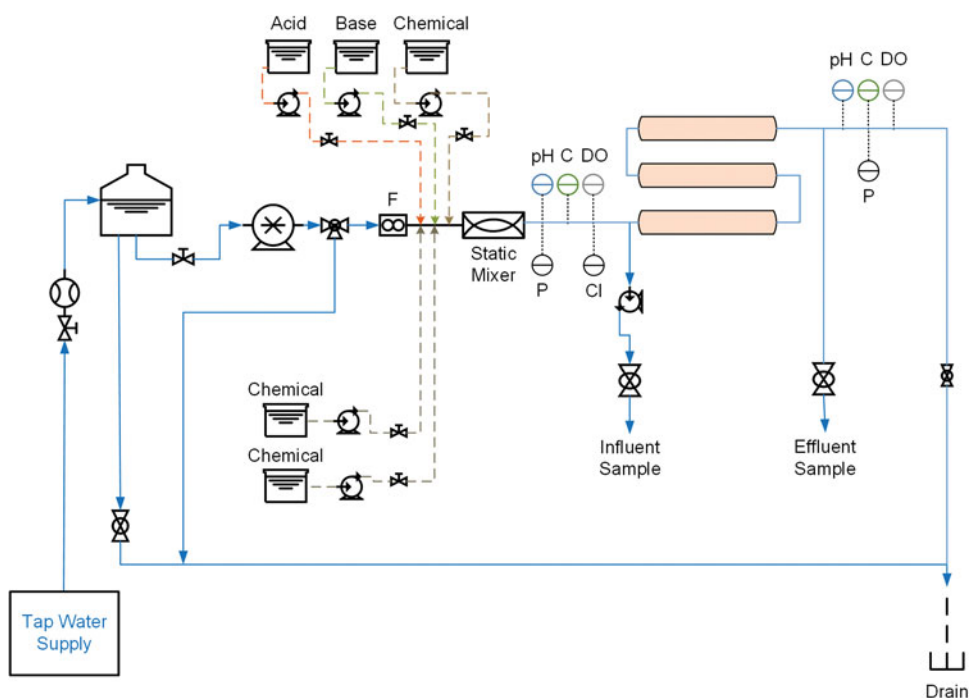


FIG. 1. Process flow diagram for the MFED system (C: electrical conductivity; DO: dissolved oxygen; Cl: free chlorine; and P: pressure). Temperature was measured by the conductivity and pH probes and the average value was reported.

$SE(\bar{d})$, was obtained using the standard deviation of the differences, $s_d \cdot SE(\bar{d}) = \frac{s_d}{\sqrt{n}}$ (n was sample size). Test statistic was computed using the standard error of the mean difference and the mean difference, $T = \frac{\bar{d}}{SE(\bar{d})}$, and under the null hypothesis, this statistic followed a test distribution with $n - 1$ degree of freedom. A test statistic was compared with the critical value of t (level of significance, $\alpha = 95\%$). When the absolute value of the calculated test statistic was larger than the critical value of t , the null hypothesis was rejected.

Results and Discussion

Changes in proton concentration and flow velocity

Irrespective of velocity, the solution pH increased significantly ($p = 0.0187$, decreasing proton concentration, Fig. 2) upon passing through the MFED magnetic field ($B = 1.350$ T). Refer to Supplementary Table S4 for all statistics related to changes in proton concentrations and electrical conductivity. As the velocity increased, the proton concentration decreased in a linear manner ($R^2 = 0.9899$). The proton concentration decreased from round 10^{-7} mol/L to around 6×10^{-8} mol/L. The observed changes in proton concentration were all greater than the mean delta values measured when the water bypassed the MFED system and were consistent over time (Supplementary Fig. S5). In addition, external pH measurements on grab samples taken from the MFED influent and effluent corroborated the changes in proton concentration measured using the in-line probes (circular symbols in Fig. 2). Therefore, the observed changes in proton concentration were not due to velocity effects, or otherwise, on the two in-line pH sensors.

Before testing the presented theoretical construct for describing the changes in proton concentrations in the MFED system, hypotheses from the literature were evaluated. Previous works have determined that solution pH, or proton concentration, may be altered in the presence of a magnetic field, and attributed this to changes in the bonding among

water molecules and the bonding between water molecule and hydronium molecule (Yamashita *et al.*, 2003). According to this hypothesis, within the magnetic field, water molecules would form more hydrogen bonds with hydronium molecules to balance the external energy provided by moving through the magnetic field.

Other possible mechanisms may be playing a role in affecting the observed changes in proton concentration. Specifically, the magnetic field may be altering the hydration characteristics of the ions present in the solution. This mechanism is captured within Coey's hypothesis, which describes how the magnetic field alters a process called prenucleation, which is the condition before nucleation of an inorganic crystal cluster (Coey, 2012). In this scenario, the prenucleation of a calcium carbonate crystal, defined by a diameter of 2 nm, is affected. As explained by the Coey's hypothesis, free protons would favor transferring to bicarbonate anions to form carbonic acid when moving through magnetic field. Therefore, the calcium carbonate crystal growth kinetics are reduced. After removal of the protons, a layer of cations could then be formed around the prenucleus. More specifically, during the growth of the prenucleus, a cation was added to the bicarbonate. The cation would then displace a proton leading to the formation of calcium carbonate. Cation displacement of the proton was hindered by the magnetic field gradient within the MFED system. As a cation passed through the magnetic field, the rate at which a cation displaced a proton decreased. The supporting mechanism for this proton displacement occurred as a result of the Lorenz Force [Equation (2)]. Coey's ecoefficiency, C [Eq. (12)], was used to quantify the potential, or likelihood, of cation displacement.

$$C = 2(L/v)f_p a \nabla B \quad (12)$$

where L is the pathway length through the gradient magnetic field; ∇B ; f_p is the Larmor frequency for a proton, 42.58 MHz/T; and a is a lattice parameter for a specific phase of calcium carbonate, for example, $a = 0.499$ nm for the calcite phase of calcium carbonate. In this study, C was >1 . When $C > 1$, the effect of the magnetic field on cation displacement would be appreciable. This means that calcium would be less able to bond with carbonate anions to form calcium carbonate. Instead, the carbonate would favor bonding with protons to form bicarbonate, or further displacement would happen. Further displacements would result in calcium remaining as free cations in solution, and the bicarbonate would bond with free protons to form carbonic acid, water, and/or carbon dioxide. Thus, the proton concentration would decrease as the protons displace the calcium. When $C < 1$, the calcium would keep bonding with carbonate and therefore, the protons would not displace the calcium and the proton concentration would not change.

Coey's coefficient could qualitatively explain why the pH would change because of the presence of ions, including calcium and magnesium, in water. However, Coey's hypothesis did not quantitatively work well in this study. According to Coey's hypothesis, when calcium, magnesium, cadmium, or zinc is present, it would lead to the displacement of carbonic acid to water and carbon dioxide. However, if it were considered that all calcium and magnesium would be displaced, the proton concentration would be less than zero

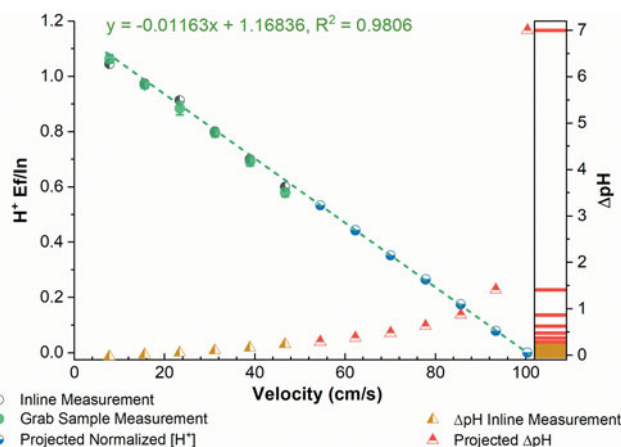


FIG. 2. Normalized proton concentration and changes in pH in the effluent from the MFED system as a function of flow velocity, and theoretical changes in proton concentration as a function of flow velocity ($B = 1.350$ T, $n = 5$, $T_{\text{avg}} = 13^\circ\text{C}$).

because the concentration of free protons would be out of mass balance (Table 1). Because the pH was initially set to pH=7, which cannot provide enough protons to be displaced. Thus, not all calcium and magnesium would be displaced. However, the Coey's hypothesis did not explain why potentially not all ions would have the displacements. Besides, Coey's hypothesis could not explain changes of proton concentration as a function of velocity.

The previously postulated hypotheses could not explain the findings in this study. In contrast, our results shown in Fig. 2 agreed with the relationship detailed in Equation (11). When the flow velocity through the magnetic field increased, so too did the amount of energy entering the water. This means that the term $-g\mu_B BNRmv$ in Equation (11) increased. Since the term $-\frac{S_0^2}{2} \sum_{ij} J_{ij}$ would not change,

$-\alpha \left(-\frac{S_0^2}{2} \sum_{ij} J_{ij} - g\mu_B BNRmv \right)$ would decrease in accordance with increasing velocity. As the influent pH was constant at 7, linearly proportional $\Delta(H^+)$ would reflect in a linearly proportional decrease in the effluent proton concentration over the influent one as a function of velocity.

With this introduced energy, $E(B)$, the structural arrangement of water molecules in solution was altered as hydrogen bonds were affected. Several scenarios are possible for free protons. Free protons may bond with water molecules to form new molecules, such as protonated water (hydronium) (Aida and Akase, 2019). Furthermore, the length of the bonding decreased/shortened when the total introduced external energy increased (Hus and Urbic, 2012). Since free protons may bond with water molecules, and the number of bonds increased in accordance with the increase in external energy, the proton concentration may decrease as velocity through the field increased (Supplementary Fig. S6). With higher bonding energy, the bond length would reduce and the hydrogen bonding structure would be altered from anticooperative to cooperative linearly. In this study, hydrogen bonding potential describes the proclivity of a water molecule, or hydronium (H_3O^+) ion, to bond with a second water molecule. Transition from an anticooperative to a cooperative condition indicates that the number of water molecules that bond with other water and/or hydronium molecules increases (Hus and Urbic, 2012; Iwata *et al.*, 2016; Aida and Akase, 2019).

According to Equation (11), as the flow velocity approaches 100 cm/s, the free proton concentration will begin to approach a value of zero, or pH=14 (Fig. 2). Beyond a ve-

locity of >100 cm/s, there may be other effects on the water properties; however, these effects are not yet captured in Equation (11). The values reported in Fig. 2 are specific to the water tested in this study. Values would differ for other systems according to the initial free proton concentration, magnetic field strength, starting energy, and water composition. Nevertheless, the same linear relationship between velocity and change in proton concentration will persist; however, the provided mechanism for changes of proton concentration in this study still could not be fully verified since the changes of energy were not yet accessible due to limited capability of current computation. For instance, the structural energy of total water molecules, $-\frac{S_0^2}{2} \sum_{ij} J_{ij}$ in

Equation (11), is not computable yet because the conditions are already beyond the bounds of current computation, for example, the number of molecules were $\gg 1,000$ (Zarmehi and Marvasti, 2017). Even considering Equations (7) and (8), arguments still existed on combination of molecular mechanics and the Newtonian mechanics (Woodhouse, 2003).

Impact of magnetic field on electrical conductivity

As with the solution pH (proton concentration), a linear relationship ($R^2=0.9833$) between changes in solution electrical conductivity and flow velocity through the MFED magnetic field was observed (Fig. 3). Also, like changes in pH, such changes in conductivity are consistent over time (Supplementary Fig. S5). In contrast to what was seen for the changes in proton concentration, the electrical conductivity from the influent to the effluent significantly increased with increasing flow velocity (Supplementary Table S4). The difference of electrical conductivity increased with flow velocity from -250 to $-100 \mu S/cm$ in accordance with the increase of velocity. As with the pH measurements, the observed changes in electrical conductivity were above those variances measured when the water was not passed through the magnetic field. Changes in electrical conductivity were further verified through grab sample analysis, indicating that the observed changes were not due to probe-specific effects.

TABLE 1. THEORETICAL PROTON REQUIREMENT FOR DISPLACING CALCIUM OR MAGNESIUM WHEN $C > 1$ AND pH=7

Ion	Concentration, mol/L
Cations	
Ca ²⁺	1.28
Mg ²⁺	0.58
Initial proton concentration	
H ⁺	10^{-7}
Protons needed for displacement	
H ⁺	$1.86 \gg 10^{-7}$

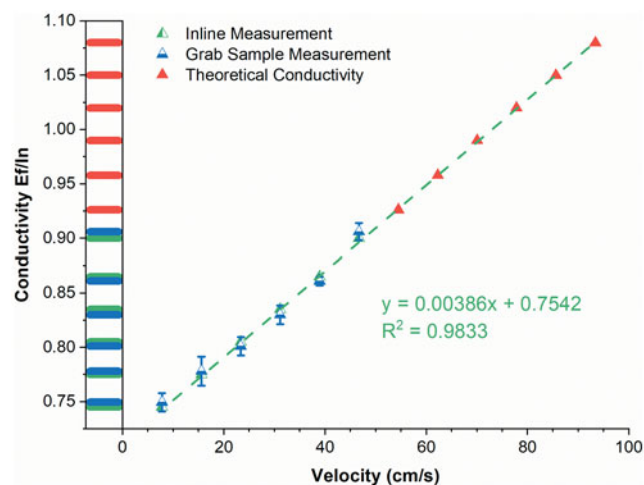


FIG. 3. Normalized changes in solution electrical conductivity upon passing through the magnetic field as a function of fluid flow velocity ($B = 1.350 T$; pH=7; $T_{avg} = 13^\circ C$; $n = 5$).

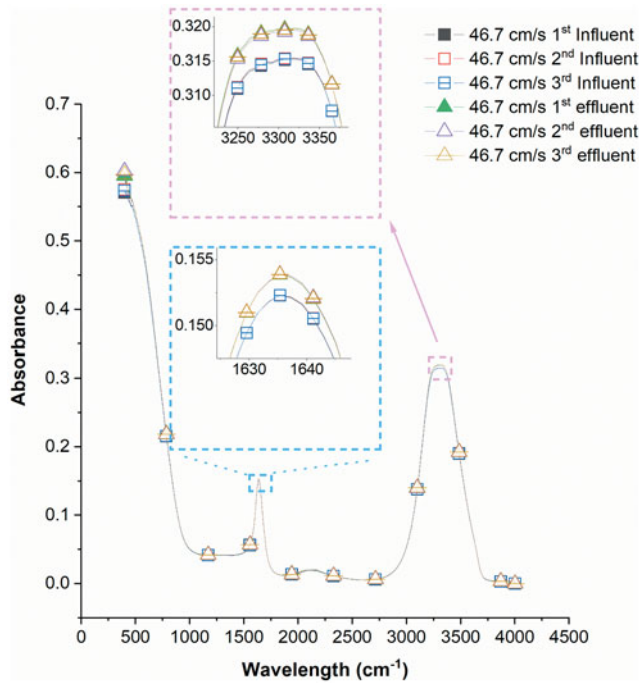


FIG. 4. FTIR spectra of water prior, and posterior, to flowing through the magnetic field at a flow velocity of 46.7 cm/s. FTIR, Fourier transform infrared spectroscopy.

Previous works have shown that the structure of the hydration shell surrounding ions is influenced/alterd by the presence of a magnetic field (Holysz *et al.*, 2007; Hus and Urbic, 2012). Differences in how this structure is altered have also been seen to be a function of whether the ion is characterized as a water structure ordering or disordering ion (Tang *et al.*, 2011; Chibowski and Szczes, 2018). The more specific changes and explanations are summarized in introduction. Holysz *et al.* (2007) observed that the change(s) in conductivity persisted up to at least 30 min even after the magnetic field was removed. This phenomenon was termed as a “memory effect” by the water and was supported by a subsequent study by Holysz *et al.* (2007). Holysz *et al.* (2002, 2007) also suggested that exposure to a magnetic field weakened the hydration shell structure of ions in solution as weakening of the hydration shells around proton, hydroxide, potassium, and chloride ions. Because the electrical conductivity of a solution is inversely proportional to the diameter of the hydrated cation and anion, and when the hydration shell is weakened or distorted by the magnetic field, the conductivity of a solution is increased (Holysz *et al.*, 2002, 2007). As was observed in the Szczes *et al.*'s (2011a) study, these researchers consistently saw an increase in solution conductivity upon exposure to a static magnetic field ($B=0.27$ T). The magnitude of the observed increase was a function of the type (water structure ordering/disordering), and concentration, of salts present in solution. The change in conductivity, assuming constant conditions, was ascribed to a change in the thickness of the water layers, or hydration shell, around a given ion in solution. This reduces the hydrated radius of the ion and results in an increase in conductivity as originally hypothesized by Higashitani *et al.* (1995).

While changes in conductivity have been previously observed in the presence of magnetic fields of different strengths, correlations to flow velocity are missing from the literature. A mechanistic description of such relationships is also missing or is incomplete. As shown in Fig. 3, the electrical conductivity increased in a linear manner with fluid velocity. This phenomenon may be described by considering the reordering of water molecules (Pang, 2006). As the energy introduced by the magnetic field and applied to a water molecule and free protons, the ordering of water molecules were changed with effects of magnetic field on hydrogen bonds. Water molecules were re-ordered from free molecules to form water molecule chain shapes within the external magnetic field. As also, the chain would contain more molecules if a stronger magnetic field was applied to the water. And the mechanism is described in introduction. The shown chains of water molecules, although did not affect hydration shell of ions to cause the changes on conductivity, such chains between water molecules would increase the ion concentration in the overall “water system.” Because as the chains of water molecules formed, they could be considered bigger molecular clusters (or bigger water molecules), and other ions such as metallic ions like calcium or nonmetallic ions like chloride would not exist in interior regions of these clusters due to steric hindrances. Therefore, as chains of water molecules were formed, the number of free water molecules in a given unit volume was reduced, and thus the ion concentration increased, leading to an increase in conductivity.

It has been reported that the relationship between velocity and alterations in hydrogen bonding is nonlinear, because of instinct nonlinear system properties (Ceriotti *et al.*, 2013). Overall, some mechanisms on effects of magnetic field on electrical conductivity have been proposed and used to explain changes in conductivity. In this study, before the conductivity ratio increased with flow velocity, the effluent conductivity was lowered relative to the influent value at $v=10$ cm/s. This decrease was explained using the mechanism provided by Szczes *et al.* (2011b). However, that theory was not enough to demonstrate the later increased conductivity as the velocity increase.

Equation (5) illustrates the roles of, and relationships between, flow velocity through a magnetic field and electrical conductivity. Since the velocity in this study was much lower than the threshold velocity, according to impact of velocity on conductivity at lower range, the conductivity introduced by moving through the magnetic field should increase in a linear manner with flow velocity (Fig. 1). The results (Fig. 3) presented a linear relationship ($R^2=0.9833$) between changes in solution electrical conductivity and flow velocity. Thus, the theory was supported by the experimental data. Therefore, the relationship,
$$\sigma = \frac{ngv_d}{\sum_n \frac{1}{4\pi\epsilon_0} \frac{q^2}{n} - vB}$$

explain changes in electrical conductivity in terms of flow velocity through a magnetic field. And the conductivity could be further predicted when the velocity is increased. For instance, in this study, if the velocity is increased to around 70 cm/s, it could be foreseen that the conductivity ration (Ef/In) would equal to one (Fig. 3). Also, with a velocity higher than 70 cm/s, the initial decrease of conductivity would potentially be counteracted, and the effluent conductivity would be higher than the influent conductivity. And if the velocity is further increased, the effluent conductivity would increase more accordingly.

Furthermore, to determine if the structuring of water molecules in solution had been altered by the MFED, FTIR absorption and NMR transverse relaxation were measured. It was found that with MFED magnetic field treatment at a flow velocity of 46.7 cm/s, the absorbance of effluent water samples was 0.05 absorbance units higher compared with the influent sample at $\lambda = 3,300 \text{ cm}^{-1}$; the absorbance of effluent samples was 0.025 higher compared with the influent sample at $\lambda = 1,600 \text{ cm}^{-1}$ (Fig. 4). Peaks at $\lambda = 3,300 \text{ cm}^{-1}$ and $\lambda = 1,600 \text{ cm}^{-1}$ are the two peaks water would present absorbance (Mojet *et al.*, 2010). When the water molecules have different structures, including forming/deforming more hydrogen bonds or molecule chains, the FTIR spectrum absorbance would change accordingly. In this case, the FTIR absorbance is increased because the hydrogen bonds increase or water molecule chains are formed (Pang, 2006; Pang and Deng, 2008). Therefore, the MFED magnetic field treatment succeeded in altering water molecules.

NMR transverse relationship (T_2 relaxation) was conducted to determine if there were more free water molecules, or more bonded water molecules through hydrogen bonds, after the MFED treatment. A shorter T_2 relaxation time means that the water molecules bonded with one another and/or other substances present in the solution relative to the untreated solution. A shorter T_2 relaxation time could also mean there are stronger hydrogen bonds between water molecules and other substances in the solution. A longer T_2 relaxation time means the water molecules are less bonded, or less tightly bonded, with other water molecules or substances (Thulborn *et al.*, 1982; Hills *et al.*, 1990; Jarymowycz and Stone, 2006; Cai *et al.*, 2009). At a flow velocity of 46.7 cm/s through the MFED, the effluent water samples had a T_2 relaxation time of $2246.21 \pm 26.06 \text{ ms}$, while the influent, or untreated, water had a longer T_2 relaxation time of $2279.81 \pm 0 \text{ ms}$. This indicates that the MFED system increased the number and/or strength of the hydrogen bonding structure of the water molecules in solution in agreement with the theoretical assessments previously discussed. With magnetic field treatment, the proportion of free water molecules declined, and/or the hydrogen bonds were strengthened. And the NMR finding in this study also agreed with the ones reported by Cai *et al.* (2009). Hence, the hypotheses in this study were supported by both the FTIR and NMR results.

Conclusions

Proton concentration and electrical conductivity were altered as a function of flow velocity through the magnetic field generated by the MFED system. Changes (decrease) in proton concentration were inversely proportional to increases in flow velocity. This decrease was due to increased hydrogen bonding between water molecules and free protons and hydronium ions. Increases in electrical conductivity were a linear function of flow velocity over the value range studied here. This was due to weakening of the hydration shells around constituent ions and increases in internal electrical field. All experimentally observed changes in proton concentration and electrical conductivity were statistically significant and reproducible. Modification of water chemistry is therefore possible in flow-through conditions, and the magnitudes of these changes may be controlled through manipulation of flow velocity. These findings demonstrate that a fundamental property, hydrogen

bonds, inherent to water systems may be manipulated using magnetic fields. This opens the door for affecting the properties and behaviors of diverse substances relevant to water/wastewater treatment, such as particle stability (coagulation) and mineral solubility. As such this work represents an important first step in reducing our reliance on chemical additives in water/wastewater treatment applications.

Author Disclosure Statement

No competing financial interests exist.

Funding Information

This work was funded by Strategic Environmental Solutions (Pensacola, FL).

Supplementary Material

Supplementary Data
 Supplementary Figure S1
 Supplementary Figure S2
 Supplementary Figure S3
 Supplementary Figure S4
 Supplementary Figure S5
 Supplementary Figure S6
 Supplementary Table S1
 Supplementary Table S2
 Supplementary Table S3
 Supplementary Table S4

References

- Aida, M., and Akase, D. (2019). Hydrogen-bond pattern to characterize water network. *Pure Appl. Chem.* 91, 301.
- Ashoori, N., Dzombak, D.A., and Small, M.J. (2017). Identifying water price and population criteria for meeting future urban water demand targets. *J. Hydrol.* 555, 547.
- Cai, R., Yang, H., He, J., and Zhu, W. (2009). The effects of magnetic fields on water molecular hydrogen bonds. *J. Mol. Struct.* 938, 15.
- Cerioti, M., Cuny, J., Parrinello, M., and Manolopoulos, D.E. (2013). Nuclear quantum effects and hydrogen bond fluctuations in water. *Proc. Natl. Acad. Sci. U.S.A.* 110, 15591.
- Chang, K.T., and Weng, C.I. (2006). The effect of an external magnetic field on the structure of liquid water using molecular dynamics simulation. *J. Appl. Phys.* 100, 043917.
- Chang, K.T., and Weng, C.I. (2008). An investigation into the structure of aqueous NaCl electrolyte solutions under magnetic fields. *Comput. Mater. Sci.* 43, 1048.
- Chibowski, E., and Szczes, A. (2018). Magnetic water treatment—A review of the latest approaches. *Chemosphere* 203, 54.
- Chibowski, E., Szczes, A., and Holysz, L. (2005). Influence of sodium dodecyl sulfate and static magnetic field on the properties of freshly precipitated calcium carbonate. *Langmuir* 21, 8114.
- Coe, J.M.D. (2012). Magnetic water treatment—How might it work? *Philos. Mag.* 92, 3857.
- Ding, S., Deng, Y., Bond, T., Fang, C., Cao, Z., and Chu, W. (2019). Disinfection byproduct formation during drinking water treatment and distribution: A review of unintended effects of engineering agents and materials. *Water Res.* 160, 313.

- Ebrahimi, S., and Saghravani, S.F. (2017). Influence of magnetic field on the thermal conductivity of the water based mixed Fe₃O₄/CuO nanofluid. *J. Magn. Magn. Mater.* 441, 366.
- Higashitani, K., Iseri, H., Okuhara, K., Kage, A., and Hatade, S. (1995). Magnetic effects on zeta-potential and diffusivity of nonmagnetic colloidal particles. *J. Colloid Interface Sci.* 172, 383.
- Hills, B.P., Takacs, S.F., and Belton, P.S. (1990). A new interpretation of proton Nmr relaxation-time measurements of water in food. *Food Chem.* 37, 95.
- Holysz, L., Chibowski, M., and Chibowski, E. (2002). Time-dependent changes of zeta potential and other parameters of in situ calcium carbonate due to magnetic field treatment. *Colloids Surf. A Physicochem. Eng. Aspects* 208, 231.
- Holysz, L., Szczes, A., and Chibowski, E. (2007). Effects of a static magnetic field on water and electrolyte solutions. *J. Colloid Interface Sci.* 316, 996.
- Hus, M., and Urbic, T. (2012). Strength of hydrogen bonds of water depends on local environment. *J. Chem. Phys.* 136, 144305.
- Iwata, S., Akase, D., Aida, M., and Xantheas, S.S. (2016). Electronic origin of the dependence of hydrogen bond strengths on nearest-neighbor and next-nearest-neighbor hydrogen bonds in polyhedral water clusters (H₂O)(n), n = 8, 20 and 24. *Phys. Chem. Chem. Phys.* 18, 19746.
- Jarymowycz, V.A., and Stone, M.J. (2006). Fast time scale dynamics of protein backbones: NMR relaxation methods, applications, and functional consequences. *Chem. Rev.* 106, 1624.
- Kusminskiy, S.V. (2019). *Quantum Magnetism, Spin Waves, and Optical Cavities*. New York City, NY, USA: Springer Briefs in Physics, p. 34.
- Levitt, M., Hirschberg, M., Sharon, R., Laidig, K., and Daggett, V. (1997). Calibration and testing of a water model for simulation of the molecular dynamics of proteins and nucleic acids in solution. *J. Phys. Chem. B* 101, 5051.
- Liu, Y., Pan, L.M., Liu, H.B., Chen, T.M., Yin, S.Y., and Liu, M.M. (2019). Effects of magnetic field on water electrolysis using foam electrodes. *Int. J. Hydrog. Energy* 44, 1352.
- Luengo-Kovac, M. (2017). Investigation of Current Induced Spin Polarization in III-V Semiconductor Epilayers. A dissertation submitted in partial fulfillment of the requirements for the degree of Doctor of Philosophy (Physics) in the University of Michigan, p. 47.
- Mojet, B.L., Ebbesen, S.D., and Lefferts, L. (2010). Light at the interface: The potential of attenuated total reflection infrared spectroscopy for understanding heterogeneous catalysis in water. *Chem. Soc. Rev.* 39, 4643.
- Pang, X.F. (2006). The conductivity properties of protons in ice and mechanism of magnetization of liquid water. *Eur. Phys. J. B* 49, 5.
- Pang, X.F., and Deng, B. (2008). Investigation of changes in properties of water under the action of a magnetic field. *Sci. China Ser. G Phys. Mech. Astron.* 51, 1621.
- Pang, X.F., and Feng, Y.P. (2003). Mobility and conductivity of the proton transfer in hydrogen-bonded molecular systems. *Chem. Phys. Lett.* 373, 392.
- Quickenden, T.I., Betts, D.M., Cole, B., and Noble, M. (1971). Effect of magnetic fields on Ph of water. *J. Phys. Chem.* 75, 2830.
- Spreiter, Q., and Walter, M. (1999). Classical molecular dynamics simulation with the Velocity Verlet algorithm at strong external magnetic fields. *J. Comput. Phys.* 152, 102.
- Szczes, A., Chibowski, E., Holysz, L., and Rafalski, P. (2011a). Effects of static magnetic field on electrolyte solutions under kinetic condition. *J. Phys. Chem. A* 115, 5449.
- Szczes, A., Chibowski, E., Holysz, L., and Rafalski, P. (2011b). Effects of static magnetic field on water at kinetic condition. *Chem. Eng. Proces.* 50, 124.
- Tang, C.Y., Huang, Z.S., and Allen, H.C. (2011). Interfacial water structure and effects of Mg²⁺ and Ca²⁺ binding to the COOH headgroup of a palmitic acid monolayer studied by sum frequency spectroscopy. *J. Phys. Chem. B* 115, 34.
- Thulborn, K.R., Waterton, J.C., Matthews, P.M., and Radda, G.K. (1982). Oxygenation dependence of the transverse relaxation-time of water protons in whole-blood at high-field. *Biochim. Biophys. Acta* 714, 265.
- Wang, Y.F., Zhang, B., Gong, Z.B., Gao, K.X., Ou, Y.J., and Zhang, J.Y. (2013). The effect of a static magnetic field on the hydrogen bonding in water using frictional experiments. *J. Mol. Struct.* 1052, 102.
- Wang, Y.K., Wei, H.N., and Li, Z.W. (2018). Effect of magnetic field on the physical properties of water. *Results Phys.* 8, 262.
- Wee, S.Y., and Aris, A.Z. (2017). Endocrine disrupting compounds in drinking water supply system and human health risk implication. *Environ. Int.* 106, 207.
- Woodhouse, N.M.J. (2003). *Special Relativity*. New York City, NY, USA: Springer, p. 60.
- Wu, Y., Tepper, H., and Voth, G. (2006). Flexible simple point-charge water model with improved liquid-state properties. *J. Chem. Phys.* 124, 024503.
- Yamashita, M., Duffield, C., and Tiller, W.A. (2003). Direct current magnetic field and electromagnetic field effects on the pH and oxidation-reduction potential equilibration rates of water. 1. Purified water. *Langmuir* 19, 6851.
- Zarmehi, N., and Marvasti, F. (2017). Bounds on Discrete Fourier Transform of Random Mask. In 2017 International Conference on Sampling Theory and Applications (Sampta), Tallin, Estonia, p. 327.

Nomenclature

Abbreviations

- AC = alternating current
 DC = direct current
 Ef = effluent
 FTIR = Fourier transform infrared spectroscopy
 In = Influent
 IR = infrared
 NMR = nuclear magnetic resonance
 ORP = oxidation reduction potential, mV

Variables

- a = lattice parameter, nm
 σ = electrical conductivity, $\mu\text{S}/\text{cm}$
 μ_B = permeability, H/m
 B = strength of magnetic field, T (Tesla)
 C = Coey's coefficient
 c = speed of light in vacuum, 2.9979×10^8 m/s
 E = electric field, V
 $E(B)$ = energy provided by a magnetic field, J
 F = Lorentz force, N
 f_p = Larmor frequency for a proton, 42.58 MHz/T
 g = dimensionless magnetic moment, $\text{kg}/(\text{m}^2 \cdot \text{s}^2)$

J_{ij} = Exchange coefficient
 L = pathway length through the gradient magnetic field, cm
 m = mass, kg
 N = number of the lattice sites
 p = linear momentum in Newtonian mechanics, kg/(m·s)
 q = the charge of particles, C (Coulomb)
 r = force between two charged substance, N
 R = radius of rotation, cm
 S = total angular momentum, kg/(m²·s)
 S_0 = instant angular momentum, kg/(m²·s)
 u = vector of unit length aligned along the force directed
 from one particle to another

v = velocity, cm/s
 ΔB = magnetic field gradient, T
 ϵ_0 = absolute dielectric constant of water, 8.85×10^{-12} F/m
 (farad per meter)

Units

cm/s = centimeters per second
 K = Kelvin, an SI base unit of thermodynamic temperature
 M = molar, mol/L (1,000 mol/m³)
 T = Tesla
 $\mu\text{S/cm}$ = micro Siemens per centimeter